

Jahn-Teller distortions and excitation energies in C_{60}^{n+}

Martin Lueders^{1,2} and Nicola Manini^{1,3,4y}

¹ International School for Advanced Studies (SISSA),
Via Beirut 4, 34014 Trieste, Italy

² INFN Democritos National Simulation Center,
and INFN, Unità Trieste, Italy

³ Dip. Fisica, Università di Milano, Via Celebria 16, 20133 Milano, Italy

⁴ INFN, Unità di Milano, Milano, Italy

Abstract

Based on previously computed parameters for the electron-phonon couplings and the Coulomb exchange, we compute and classify the static Jahn-Teller distortions, i.e. the minima of the lowest adiabatic potential energy surface, of C_{60}^{n+} , for all values of charge $1 \leq n \leq 9$ and spin. We compute the intra-band electronic excitation energies in the different optimal geometries in the sudden approximation, and find a spread of the electronic states of roughly 1 eV. We also obtain the leading vibronic quantum corrections to the ground-state energy, equal to zero-point energy lowering due to the softening of the phonons at the adiabatic Jahn-Teller minima: these non-adiabatic corrections are so large that for $4 \leq n \leq 6$ states of different spin symmetry turn lower than the high-spin adiabatic ground state.

E-mail: lueders@sisssa.it

^yE-mail: nicola.manini@mil.infn.it

1 Introduction

Low-spin states are associated to larger distortions, thus larger energy gains, than high-spin states in degenerate electron-phonon coupled molecules and impurity centers. Electron-electron Coulomb repulsion opposes this tendency, favoring high-spin states instead, in accord to the first of Hund's rules. The Jahn-Teller (JT) systems C_{60}^{n+} are no exception to this rule: if electron-phonon coupling was the only relevant interaction, then the n -holes ground state would be either of spin $S = 0$ (even n) or $S = \frac{1}{2}$ (odd n). As was recently shown [1], in positive fullerene ions the size of Coulomb interaction is sufficiently large to enforce Hund's rule: the ground states of C_{60}^{n+} was calculated to always be high spin ($S = \frac{n}{2}$ for $n \leq 5$, $S = \frac{10-n}{2}$ for $n > 5$) in the adiabatic approximation. This result is confirmed for $n = 2$ by NMR investigation of solid-state compounds [2]. The JT distortions in C_{60}^{n+} , though strongly counteracted by the larger electron-electron repulsion, yet represent an important, and still largely unexplored, contribution to the energetics of C_{60}^{n+} . Investigation of this contribution, and in particular of the corrections to the adiabatic approximation, is the main subject of this work.

The JT model relevant for C_{60}^{n+} is conventionally indicated as $h^n (A + G + H)$, where h refers to the n -fold-degenerate highest occupied molecular orbital (HOMO), and A, G, H refer to the 2 nondegenerate A_g , 6 fourfold-degenerate G_g and 8 n -fold-degenerate H_g molecular vibration modes that are linearly coupled to the h_u states according to icosahedral symmetry [1, 3, 4]. We investigate this model by treating the normal coordinates for these vibrational modes as classical variables, and searching the minima of the adiabatic potential energy surface in the 66-fold dimensional space of these distortions. Each of these static JT configurations is characterized by a reduced symmetry from icosahedral to some (usually) lower symmetry. New vibrational frequencies arise at these local minima: we determine these frequencies by evaluation of the Hessian matrix at the minimum [5]. The lowering of the vibrational frequencies gives the leading quantum correction to the adiabatic approximation. The original icosahedral symmetry of the problem is restored once the presence of several equivalent optimal distortions is recognized, and quantum tunneling between these wells is allowed. Proper accounting of tunneling gives the next-order quantum correction, but in the present work, we limit ourselves to the study of the local properties of the wells and the connectivity of the sets of minima in distortion space, for all values of charge n and spin S .

The competing intra-molecular exchange of Coulomb origin and the JT interaction both contribute to the computed spectrum of excitations. Differences in energies of the fully relaxed configurations at different spin compare directly

with spin gaps as could be measured in "slow" spectroscopies such as electron or nuclear magnetic resonance. In contrast, the electronic excitation energies computed keeping the molecular geometry fixed in the lowest minimum compare directly with the vertical excitations probed by fast optical spectroscopies. Both these class of quantities are reported in this work.

This paper is organized as follows: Sec. 2 introduces the model and the parameters used in this calculation, which is then described in Sec. 3, along with the properties of the JT minima for all values n and S ; Sect. 4 contains the vertical excitation spectra. The the zero-point non-adiabatic corrections are described in Sec. 5. The results are discussed in Sec. 6, and connectivity matrices are collected in an Appendix.

2 The model Hamiltonian

We report here for completeness the model Hamiltonian previously introduced in Ref. [1] to describe the physics of the holes in the h_u HOMO of C_{60} fullerene:

$$\hat{H} = \hat{H}_0 + \hat{H}_{\text{vib}} + \hat{H}_{\text{ev}} + \hat{H}_{\text{ee}} \quad (1)$$

where

$$\hat{H}_0 = \sum_m \hat{c}_m^\dagger \hat{c}_m \quad (2)$$

$$\hat{H}_{\text{vib}} = \sum_i \frac{\hbar \omega_i}{2} (\hat{P}_i^2 + \hat{Q}_i^2) \quad (3)$$

$$\hat{H}_{\text{ev}} = \sum_{ri} \frac{\kappa g_i^r \hbar \omega_i}{2} \sum_{m m^0} C_{m m^0}^r \hat{Q}_i \hat{c}_m^\dagger \hat{c}_{m^0} \quad (4)$$

$$\hat{H}_{\text{ee}} = \frac{1}{2} \sum_{\substack{m m^0 \\ n n^0}} \sum_{\substack{m' m'^0 \\ n' n'^0}} w_{; 0} (m; m^0; n; n^0) \hat{c}_m^\dagger \hat{c}_{m^0}^\dagger \hat{c}_{n^0} \hat{c}_n \quad (5)$$

are respectively the single-particle Hamiltonian, the vibron contribution (representing the phonon kinetic energy plus the restoring potential expanded to quadratic order around the equilibrium configuration of neutral C_{60}), the electron-vibron coupling (in the linear JT approximation) [4, 6], and finally the mutual Coulomb repulsion between the electrons. The \hat{c}_m^\dagger denote the creation operators of a hole in the HOMO, described by the single-particle wave function $\psi_m(r)$. \uparrow indicates the spin projection; m and n label the component within the fivefold degenerate electronic HOMO multiplet, based on the C_5 quantum number m from the $I_h \supset D_5 \supset C_5$ group chain [4, 7]. i counts the phonon modes of symmetry ($2 A_g$, $6 G_g$ and $8 H_g$ modes). $C_{m m^0}^r$ are

	$\hbar \omega_i$	$\hbar \omega_i$	g_i	θ_i	$E_s(D_5)$	$E_s(D_3)$
	cm ⁻¹	meV		deg	meV	meV
A_g						
	500	62.0	0.059	–	0.0	0.0
	1511	187.4	0.274	–	1.8	1.8
G_g						
	483	59.9	0.757	–	0.0	1.9
	567	70.3	0.102	–	0.0	0.0
	772	95.7	0.800	–	0.0	3.4
	1111	137.8	0.624	–	0.0	3.0
	1322	163.9	0.228	–	0.0	0.5
	1519	188.4	0.467	–	0.0	2.3
H_g						
	261	32.4	3.042	0:1	30.0	0.0
	429	53.2	1.223	30:1	6.0	1.1
	718	89.0	0.995	89:4	0.0	4.9
	785	97.3	0.784	2:3	6.0	0.0
	1119	138.7	0.221	76:6	0.0	0.4
	1275	158.0	0.519	28:0	3.3	0.5
	1456	180.5	0.962	28:1	13.0	2.1
	1588	196.9	0.869	31:1	10.9	2.2

Table 1: Computed mode eigenfrequencies and e-v linear coupling parameters of the h_u HOMO in C_{60} [6]. The classical single-mode JT stabilization energies E_s are tabulated for both D_5 and D_3 distortions, for one hole in the HOMO.

Clebsch-Gordan coefficients [7] of the icosahedral group I_h , for coupling two h_u states to phonons of symmetry Γ . r is a multiplicity label, relevant for modes of $\Gamma = H_g$ symmetry only [6, 7]. \hat{Q}_i are the molecular normal mode vibration coordinates (measured from the adiabatic equilibrium configuration of C_{60}), and \hat{P}_i the corresponding conjugate momenta. Spin-orbit is exceedingly small in C_{60} [8] and it is therefore neglected.

The electron-vibron (e-v) couplings g_i^r are conveniently expressed in units of the corresponding harmonic vibron quantum of energy $\hbar \omega_i$. In this calculation we adopt the numerical values of the e-v coupling parameters, listed in Table 1, from the Density Functional (DF) calculation of Ref. [6], and a second calculation [9] yields couplings in substantial accord with those of Table 1. The numerical factors $k^{A_g} = 5^{\frac{1}{2}}$, $k^{G_g} = \frac{5}{4}^{\frac{1}{2}}$, $k^{H_g} = 1$ in \hat{H}_{e-v} have been introduced for compatibility with the normalization of Ref. [6].

Parameter	Value [meV]	
F ₁	15646	9
F ₂	105	10
F ₃	155	4
F ₄	47	5
F ₅	0	3
U	3097	1

Table 2: The Coulomb parameters for C_{60}^{n+} , as obtained from the DF calculations of Ref. [1]. One of the tabulated parameters (e.g. F_1) is a linear combination of the five others.

The Coulomb matrix elements are defined by:

$$w_{;0}(m; m^0; n; n^0) = \int d^3r \int d^3r^0 u_{;0}(r; r^0) u_{;0}(r; r^0) u_{;0}(r; r^0) u_{;0}(r; r^0) u_{;0}(r; r^0) \quad (6)$$

where $u_{;0}(r; r^0)$ is an effective Coulomb repulsion, screened by the other electrons of the molecule. Detailed symmetry analysis shows [1] that, assuming spin-independence of the orbitals, this set of coefficients can be expressed as

$$w_{;0}(m; m^0; n; n^0) = \sum_{r;r^0} F^{r;r^0} \prod_{m,n} C_{m,n}^r C_{m^0,n^0}^{r^0} \quad (7)$$

in terms of a minimal set of independent parameters $F^{r;r^0}$. A DF calculation of these parameters was carried out in Ref. [1], and for our calculation we adopt those values of the Coulomb parameters, which we report for completeness in Table 2. For the Coulomb parameters we use the shorthands

$$F_1 = F^{A_g}; F_2 = F^{G_g}; F_3 = F^{1;1;H_g}; F_4 = F^{2;2;H_g}; F_5 = F^{1;2;H_g}; \quad (8)$$

and the combination

$$U = \frac{F_1}{5} - \frac{4F_2}{45} - \frac{F_3}{9} - \frac{F_4}{9} : \quad (9)$$

U defines an average Coulomb repulsion within the n -holes multiplets, so that

$$E^{ave}(n) = \text{Tr}_n(\hat{H}_0 + \hat{H}_{ee}) = n + U \frac{n(n-1)}{2} : \quad (10)$$

It should be noted that U differs from the usual definition of the Hubbard U, involving the lowest multiplet in each n -configuration: $U^{min} = E^{min}(n+1) + E^{min}(n-1) - 2E^{min}(n)$. This second definition is inconvenient here, since it depends wildly on n .

n	S	adiabatic	vibrational	electronic
2	0	-129	270	-399
	1	-142	99	-241
3	1/2	-168	267	-435
	3/2	-222	99	-320
4	0	-200	361	-561
	1	-211	229	-440
	2	-308	69	-377
5	1/2	-203	308	-511
	3/2	-256	169	-425
	5/2	-397	0	-397

Table 3: The total adiabatic energy $V^{\text{ad}}(Q_{\text{min}})$ (in meV) of the lowest electronic state for each n and S , including the e-e and e-v contributions from $\hat{H}_{\text{vib}} + \hat{H}_{\text{e-v}} + \hat{H}_{\text{e-e}}$ (but excluding the $[U_n(n-1)=2]$ term), for C_{60}^{n+} . The last two columns distinguish the vibrational (\hat{H}_{vib}) and electronic ($\hat{H}_{\text{e-v}} + \hat{H}_{\text{e-e}}$) contributions.

3 The adiabatic calculations

We approximate the vibron operators \hat{Q}_i with classical coordinates, in the spirit of the adiabatic approximation. In an orbitally degenerate situation (as for the C_{60}^{n+} ions at hand) the adiabatic approximation usually yields fairly accurate energetics in the limit of large the e-v couplings, so that tunneling between equivalent minima can safely be neglected [10]. The phonon kinetic term in (3) is neglected in the adiabatic approximation. In Sect. 5 we will partly restore this term by taking into account quantum zero-point energies. In any classical statically JT-distorted configuration, the icosahedral symmetry is broken: therefore states of different icosahedral symmetry representations are inter-mixed. Only the total number of holes n , total spin S and its projection S_z are conserved upon distortion. Here, we neglect any change of the Coulomb Hamiltonian upon distortion, and we assume therefore that $\hat{H}_{\text{e-e}}$ is still determined according to Eqs. (5,6,7) by the same parameters F_i of Table 2, as in icosahedral symmetry. Also, we assume no change of the phonon frequencies ω_i and couplings g_i^r upon charging.

For each n, S and M_S , we allow the 64 ($6 \times 4 G_g$ plus $8 \times 5 H_g$) phonon coordinates to relax, and determine the optimal distortion, by full minimization

of the lowest adiabatic potential sheet $V^{\text{ad}}(Q)$ in the space of all the phonon coordinates Q . We leave the A_g modes out, since they contribute a trivial

$$E^{A_g}(n) = \frac{1}{8} n^2 \sum_i g_{iA_g}^2 \hbar^2 = n^2 \cdot 1.79 \text{ meV}; \quad (11)$$

spin- and symmetry-independent term to the energetics. Because of particle-hole symmetry, charges $n > 5$ can always be reduced to the computed charges $n < 5$. In Table 3, we report the resulting optimally-distorted energy in each spin sector, based on the electron-electron (e-e) and e-v couplings of C_{60}^{n+} ions, as previously published in Ref. [1]. The main outcome of the adiabatic calculation is that positive C_{60} ions favor high-spin ground states (contrary to the analogous finding for negative ions).

In the present contribution, we extend the previous calculation to obtain the complete set of all the equivalent minima for each $(n;S)$ sector. To this purpose, we generate about a hundred randomly distributed distortions away from the I_h high-symmetry point, and let the molecule relax to the closest minimum, by combined standard (simplex and conjugate-gradients) minimization algorithms. We then apply the symmetry operations of the icosahedral group to the each of the minima found, in order to locate any possibly missing minimum. Although the method employed is not deterministic, the symmetry analysis makes the probability that any set of minima is incomplete utterly negligible. Thus, for each n and S we obtain a complete set of equivalent global minima. In the few cases where the minimization leads to non-global minima, we have discarded them based on simple comparison of the adiabatic energies.

In Table 4 we summarize some global properties of the obtained JT minima for all charge and spin states. In these multimode JT systems, the local symmetry of an optimal distortion is described in terms of the subgroup G_{local} of symmetry operations which leave that minimum invariant. We remind that the minima in the $n = 1, S = \frac{1}{2}$ case, where e-e interaction is unimportant, were found to be 6, of local D_{5d} symmetry [3, 4, 6]. For $2 \leq n \leq 8$, where the role of e-e interaction is crucial, the number of JT minima follows from the local symmetry: it is generally given by the ratio $|I_h|/|G_{\text{local}}|$ of the orders of the icosahedral group (120) and of the invariant subgroup.

Special care has to be taken for $n = 5$ holes. Here, in addition to the icosahedral symmetry, the system is particle-hole symmetric, i.e. invariant under exchange of fermion creation and annihilation operators. This transformation leaves the Coulomb Hamiltonian \hat{H}_{e-e} invariant, while the vibron interaction \hat{H}_{e-v} is unchanged provided that a sign change of the vibron coordinates \hat{Q}_i ; is also performed. Hence, for a given minimum Q_{min} , also its opposite

n	S	number of minima	local symmetry	number of 1 st , 2 nd , 3 rd ... neighbors	distortion $Q_{\text{min } j}$
2	0	6	D _{5d}	5	3.12
	1	15	D _{2h}	4 4 4 2	1.87
3	1/2	30	C _{2v}	2 1 2 4 4 2 2 2 4 4 2	3.08
	3/2	15	D _{2h}	4 4 4 2	1.87
4	0	10	D _{3d}	3 6	3.52
	1	30	C _{2v}	2 2 2 2 1 4 4 4 6 2	2.85
	2	6	D _{5d}	5	1.58
5	1/2	60	C _{2v}	1 2 2 4 4 4 2 2 2 4 2 2 4 2 2 2 4 4 4 2 2 1 1	3.27
	3/2	30	C _{2v}	8 12 8 1	2.46
	5/2	1	I _h	0	0

Table 4: The number and the local symmetries of the JT minima for given charge n and spin S . In the 5th column the number of neighbors of all orders are listed for a given minimum. The last column gives the total amount of dimensionless JT distortion at each minimum.

Q_{min} is a minimum of the potential energy surface. In the case $n = 5$ $S = \frac{1}{2}$, this leads to a doubling of the minima: the local C_{2v} symmetry would lead to 30 minima, but 30 more equivalent minima are added in the opposite positions by particle-hole symmetry. For $n = 5$ $S = \frac{3}{2}$ instead, the number of minima remains 30, since for each minimum there is one of the I_h symmetry operations that transforms this minimum into its opposite point. Note that this operation is not the spatial inversion (since all vibrations considered here form even representations), which are invariant under inversion, but a twofold rotation. Finally, for $n = 5$ $S = \frac{5}{2}$, the electronic state is orbitally nondegenerate, thus no JT distortion takes place.

Table 5 collects some quantitative information about the contribution of each mode to the amount of JT distortion at each minimum. As expected, the largest distortion involves always the lowest H_g mode, which is the most strongly coupled one (see Table 1). Also, the D₅ distortions receive no contribution of the G_g modes, which contribute to all the lower-symmetry minima instead.

Table 4 contains some information about the connectivity of the minima in Q space. In some cases, the specification of the number of first, second, etc.

n	S	Symmetry	distortions of G _g and H _g modes (dimensionless)								
2	0	D _{5d}	0.00	0.00	0.00	0.00	0.00	0.00	0.00	0.00	0.00
			2.69	0.935	0.0095	0.692	0.0455	0.405	0.749	0.657	
2	1	D _{2h}	0.0755	0.0102	0.0799	0.0623	0.0227	0.0466			
			1.58	0.611	0.138	0.404	0.0516	0.262	0.486	0.346	
3	1/2	C _{2v}	0.0548	0.0074	0.0580	0.0452	0.0165	0.0339			
			2.62	1.01	0.185	0.669	0.0799	0.433	0.801	0.571	
3	3/2	D _{2h}	0.0755	0.0102	0.0799	0.0623	0.0227	0.0466			
			1.58	0.611	0.138	0.404	0.0516	0.262	0.486	0.346	
4	0	D _{3d}	0.0828	0.0112	0.0877	0.0683	0.0249	0.0512			
			2.88	1.30	0.494	0.728	0.153	0.553	1.02	0.486	
4	1	C _{2v}	0.074	0.010	0.0782	0.061	0.0223	0.0457			
			2.39	0.968	0.228	0.609	0.0879	0.414	0.767	0.486	
4	2	D _{5d}	0.00	0.00	0.00	0.00	0.00	0.00			
			1.36	0.473	0.0046	0.35	0.023	0.205	0.379	0.333	
5	1/2	C _{2v}	0.101	0.0135	0.106	0.0827	0.0302	0.0619			
			2.70	1.17	0.401	0.683	0.129	0.50	0.926	0.492	
5	3/2	C _{2v}	0.0384	0.0053	0.0411	0.032	0.0117	0.024			
			2.12	0.756	0.0391	0.544	0.0427	0.327	0.605	0.503	
5	5/2	I _h	0.00	0.00	0.00	0.00	0.00	0.00			
			0.00	0.00	0.00	0.00	0.00	0.00	0.00	0.00	0.00

Table 5: The JT distortion at the minima, for each mode and value of the charge n and spin S . The distortions \hat{D}_{ij} are given in units of the length scale $x_0(i) = \sqrt{\hbar/(m_C \omega)}$ associated to each harmonic oscillator (m_C is the mass of the C atom). The $x_0(i)$ for the G_g and H_g modes of C₆₀ are: 76.3, 70.4, 60.3, 50.3, 46.1, 43.0; 103.7, 80.9, 62.6, 59.8, 50.1, 47.0, 43.9, 42.1 pm, respectively.

neighbors of a given minimum is sufficient to clarify completely the topology of the minimum in the 64-dimensional space. In particular, the D_{5d} wells of both the $n = 2, S = 0$ and the $n = 4, S = 2$ surfaces are located on the six vertices of the 5d-dimensional regular simplex, the generalization of a tetrahedron, each minimum being equally distant from all the others: this is analogous to the previously determined minimum of V^{ad} for $n = 1, S = \frac{1}{2}$ [4]. In analogy, the connectivity of the 10 D_{3d} minimum for $n = 4, S = 0$ is the same of the one depicted in Fig. 1b of Ref. [4].

For the other cases of lower symmetry, the number of neighbors of any given order must be complemented by some extra connectivity information. First, we observe that the minimum for $n = 2, S = 1$ and for $n = 3, S = \frac{3}{2}$ are exactly the same. Indeed, these two cases are related by a particle-hole symmetry applied only to one spin flavor. For all nonequivalent cases, the complete topological information about the wells is contained in the connectivity matrix $C(n; S)_{ij}$, whose matrix elements indicate that minimum i and j are $C(n; S)_{ij}$ th neighbors. We report those matrices in the Appendix. Careful examination of $C(n; S)$ for $n = 2, S = 1$ and $n = 3, S = \frac{3}{2}$ shows that each of the 15 minimum is linked to four nearest neighbor minimum, which, in turn, are linked to more minimum, forming a completely connected regular polytope. The matrices $C(3; \frac{1}{2})$ and $C(4; 1)$, show that, for $n = 3, S = \frac{1}{2}$ and $n = 4, S = 1$, the 30 minimum are divided into 6 pentagonal "clusters" of five nearest-neighboring minimum. In contrast, for $n = 5, S = \frac{1}{2}$, nearest-neighbor wells come in pairs. Finally, the 30 minimum for $n = 5, S = \frac{3}{2}$, show the largest connectivity, and sit at the vertices of a highly symmetric polytope.

4 Vertical excitation energies

In Table 6 we report the range of "vertical" excitation energies E for all natural spin symmetries S^0 , in the frozen minimum configurations $Q_{min}(n; S)$, for all values of n and S . The complete spectrum (available upon request from the authors) is very dense and not much informative. The listed energies give a quantitative prevision of the spectral range where a fast (optical) spectroscopy is likely to locate the intra-band HOMO excitations of the C_{60}^{n+} ions. For the experimentally most accessible case $n = 2, S = 1$, here follows the complete list of the triplet-triplet excitation energies: 127, 149, 150, 178, 182, 218, 326, 337, and 346 meV.

m in i m u m		exc. states	$E^{m in}$	$E^{m ax}$
n	S	S^0	[m eV]	[m eV]
2	0	0	221	823
		1	140	507
	1	0	75	635
		1	127	346
3	1/2	1/2	132	918
		3/2	99	619
	3/2	1/2	125	784
		3/2	127	346
4	0	0	192	1464
		1	102	1141
		2	165	509
	1	0	82	1232
		1	120	881
		2	54	408
4	2	0	234	981
		1	163	647
		2	167	179
5	1/2	1/2	128	1320
		3/2	74	805
		5/2	114	-
	3/2	1/2	120	997
		3/2	143	693
		5/2	28	-
	5/2	1/2	316	731
		3/2	203	377
		5/2	-	-

Table 6: The lowest and highest vertical excitation energies (in m eV) calculated assuming that the C_{60}^{n+} ion remains frozen in one of the adiabatic minima when the electronic state is excited. The first two columns are the relevant distortion. The third column indicates the spin S^0 of the excited states considered. The excitation energies in the last two columns are referred to the adiabatic energy of each specific minimum, reported in Table 3.

5 Non-adiabatic corrections

The leading quantum correction to the static JT energetics is given by the zero-point energy gain due to the softening of the vibrational frequency at the JT-distorted minimum [5]. To obtain this information, by finite differences we compute the Hessian matrix of the second-order derivatives of the lowest adiabatic potential sheet, at one of the static JT minimum Q_{min}

$$H_{fi} = \frac{\partial^2 V^{ad}(Q)}{\partial Q_i \partial Q_i} \Big|_{Q_{min}} \quad (12)$$

The vibrational frequencies ω_j at the distorted point are the eigenvalues of the Hessian matrix. There is no square root involved in the ω_j , as the coordinates are scaled with the harmonic length scale x_0 (defined in Table 5). In the harmonic approximation, these "new" normal mode frequencies ω_j contribute a zero-point energy $\frac{1}{2} \hbar \omega_j$ to that minimum configuration: the difference between this and the original zero-point energy $\frac{1}{2} \hbar \omega_i$ gives the leading quantum correction

$$E_{zero}(n;S) = \frac{1}{2} \sum_j \hbar \omega_j(n;S) - \frac{1}{2} \hbar \omega_i \quad (13)$$

to the classical energy. We rewrite this correction as

$$\begin{aligned} E_{zero}(n;S) &= \frac{1}{2} \sum_j \hbar H_{fi}(n;S) \omega_j \\ &= \frac{1}{2} \text{tr} V^{ad}(Q) \Big|_{Q_{min}} \sum_i \hbar \omega_i \quad (14) \end{aligned}$$

using the invariance of the trace under change of basis.

Table 7 displays the lowest adiabatic energies for given charge and spin in various approximations. The first column reports the adiabatic energy, $E_{class} = V^{ad}(Q_{min})$, as in Table 3. The zero-point energy corrections in the following column are comparable in magnitude to the leading adiabatic energies. In particular the very large values of zero-point energy gain for $n = 5, S = \frac{1}{2}$ is associated to very shallow minima, connected by low barriers. The lowest vibrational frequency is as small as $\omega_1 = 2.3$ meV. In the rather close competition between the Coulomb physics (Hund's rules) and the JT physics (anti-Hund behavior) the zero-point correction is very important, and, as shown by the last column of Table 7, reduces drastically the spin-gap ($n = 3$), or even changes the ground-state symmetry in favor of an intermediate ($n = 4$) or low ($n = 5$) spin state.

n	S	E_{class}	E_{zero}	$E_{\text{class}} + E_{\text{zero}}$
2	0	-129	-125	-254
	1	-142	-159	-301
3	1/2	-168	-207	-376
	3/2	-222	-159	-380
4	0	-200	-213	-412
	1	-211	-227	-437
	2	-308	-93	-400
5	1/2	-203	-247	-449
	3/2	-256	-175	-431
	5/2	-397	0	-397

Table 7: The total adiabatic energy $E_{\text{class}} = V^{\text{ad}}(Q_{\text{min}})$ (in meV) of the lowest electronic state for each n and S , including the e-v and e-e contributions from $\hat{H}_{\text{vib}} + \hat{H}_{\text{e-v}} + \hat{H}_{\text{e-e}}$ (but excluding the $[U_n(n-1)=2]$ term), for C_{60}^{n+} . The following column contains the leading non-adiabatic correction E_{zero} , the zero-point energy defined in Eq. (14). The last column reports the adiabatic energy E_{class} corrected by the zero-point term E_{zero} : for $n=4$ it leads to a different ordering of the spin states.

The zero-point correction treated here represents the g_i^0 term of a large-coupling expansion, where the adiabatic energy E_{class} is the leading (g_i^2) term. The next corrections to be considered, of order g_i^2 , are associated to tunneling among minima, possibly affected by Berry phases [4, 11, 12]. Tunneling is likely to be especially important between the pairs of neighboring minima of the $n=5$ $S=\frac{1}{2}$ adiabatic surface. Tunneling will be dealt with in future work.

6 Discussion and Conclusions

In the present calculation both e-e and e-v interactions are included for the HOMO shell of C_{60} . E-e exchange terms are treated essentially exactly, in the assumptions that (i) inter-band couplings can be neglected, and only act as a renormalization of the Coulomb parameters and that (ii) the latter are independent of the charge n in the HOMO. In principle, due to both orbital and geometrical relaxation, the effective Coulomb interaction (6) will depend

on the instantaneous charge state of the fullerene ion. However, this effect, a very important one in single-atom calculations, is expected to be fairly small in such a large molecule as C_{60} . In a JT system, the coupled phonons should in principle be treated fully quantum mechanically, as nonadiabatic effects may be important. However for strong electron-phonon coupling, the leading terms (of order g^2) are obtained in the adiabatic approximation, by studying the minima of the lowest adiabatic potential surface $V^{ad}(Q)$. Non-adiabatic effects are taken into account to the next order (g^0) by the calculation of the new harmonic oscillation frequencies close to the adiabatic JT minima. These zero-point corrections are significantly large, and they can even reverse the theoretical prediction for the symmetry of the ground state of the C_6^{n+} ion for $4 \leq n \leq 6$. Tunneling matrix elements which mix different minima to suitable dynamical combinations restore the original icosahedral symmetry and provide the next-order (g^2) quantum correction to the energetics. These terms, which will be the subject of future work, are likely to be especially large for $n = 5$ $S = \frac{1}{2}$.

The present calculation was carried out in the linear e-v approximation. As the coupling and thus the distortions are fairly large, quadratic and higher-order (in Q) couplings and vibrations anharmonicity could be important. Unfortunately, no estimate for those higher-order couplings is available yet.

The parameters used in this calculation, both for e-e and e-v interaction are most likely underestimated by the local density approximation used in their determination, as discussed in Ref. [1, 6]. Consequently, both the Coulomb repulsion and the phonon-mediated attraction calculated within the local density approximation are likely to need a rescaling by a similar factor of order two. Indeed, the balance between the two opposing interactions is delicate in C_{60}^n ions (as demonstrated by the presence of both high-spin and low-spin local ground states in different chemical environments [13, 14, 15, 16, 17, 18, 19]). In C_{60}^{n+} e-e interaction prevails at the adiabatic level: high-spin states are favored, as experiments confirm for $n = 2$ [2]. According to our calculation, however, more highly charged states, close to HOMO half filling should favor local low-spin.

An effective local exchange interaction favoring low spin is a crucial ingredient for superconductivity in a strongly-correlated orbitally-degenerate material such as a solid of doped C_{60} [20, 21]. If screening and retardation effects could be neglected, the present single-molecule calculation suggests that superconductivity should be strongly suppressed in the hole-doped solid at doping $0 \leq n \leq 3$, but could be recovered close to half filling $4 < n < 6$. It is presently unclear if such a high level of hole doping is practically accessible, except possibly by field-induced charging [22].

A Appendix

We report here the connectivity matrices whose matrix element (ij) indicates that m_i in a_i and j are $C(n;S)_{ij}$ th neighbors, for all the nontrivial n, S cases. We include up to 9th neighbors, substituting those of higher order with a dash.

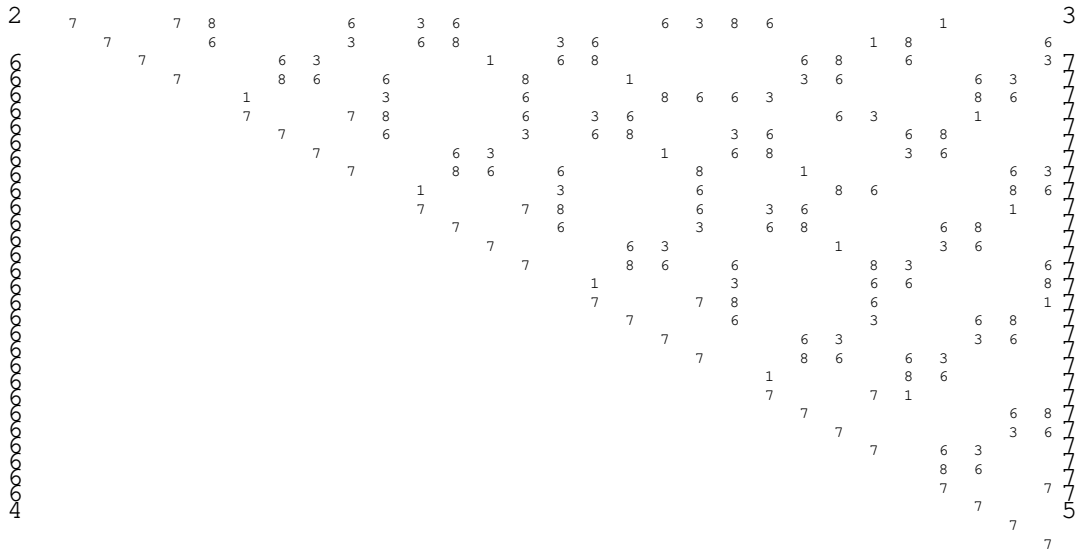
$$C(2;1) = C(3; \frac{3}{2}) = \tag{15}$$

2	4	4	2	3	1	3	2	1	1	2	3	3	1	2	3
6		4	3	1	2	1	3	2	2	3	1	1	2	3	7
6			1	2	3	2	1	3	3	1	2	2	3	1	7
6				4	4	3	2	1	2	3	1	2	3	1	7
6					4	1	3	2	3	1	2	3	1	2	7
6						2	1	3	1	2	3	1	2	3	7
6							4	4	1	2	3	2	3	1	7
6								4	3	1	2	3	1	2	7
6									2	3	1	3	1	2	7
6										4	4	2	3	1	7
6											4	3	1	2	7
6												1	2	3	7
6													4	4	7
6														4	5

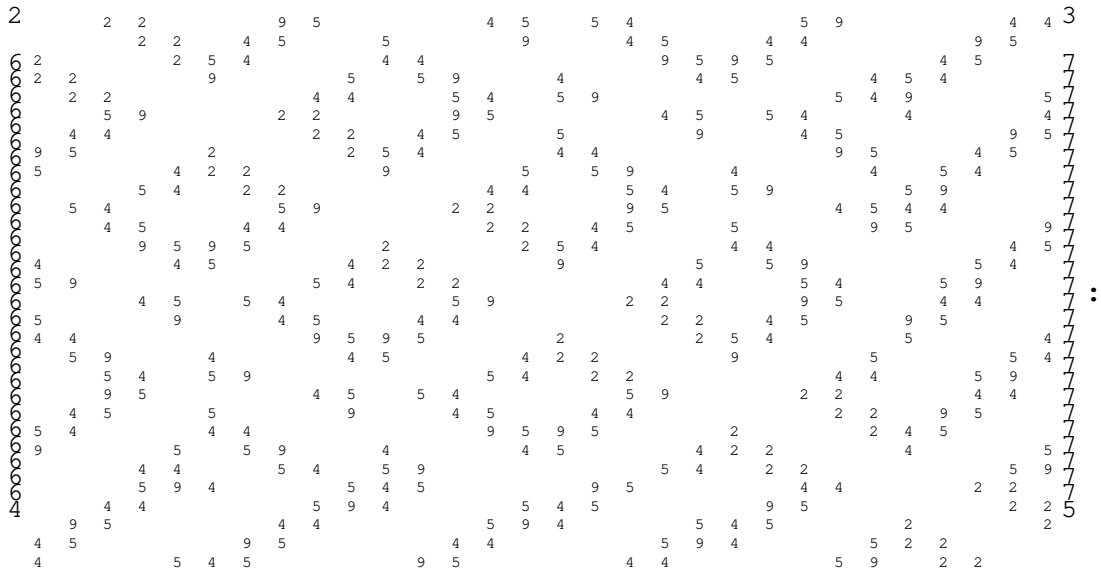
$$C(3; \frac{1}{2}) = \tag{16}$$

2	2	6	3	5	9	3	5	9	5	8	9	7	1	5	4	8	9	1	7	4	4	6	4	3												
6		4	5	9	8	1	6	9	4	5	4	7	5	1	8	6	9	5	9	5	1	4	7	8	3	5	3	2	7	8						
6			5	9	4	1	7	3	6	4	5	4	7	5	4	3	6	9	4	5	6	1	4	3	6	1	4	3	6	1						
6				9	4	5	7	8	9	5	7	8	3	9	5	4	3	6	9	5	1	9	8	4	7	5	7	3	2	7						
6					2		2	5	3	9	8	4	1	9	7	4	8	5	7	9	1	5	6	4	3	9	4	9	8	6	9					
6						2		4	8	9	1	4	3	5	6	9	5	1	9	8	4	7	5	7	9	4	9	4	9	4	9					
6							2		5	1	4	7	7	9	8	5	1	5	6	4	3	9	4	9	8	6	9	4	9	4	9					
6								2	3	4	6	5	5	9	3	4	9	7	4	1	5	8	6	9	4	1	5	4	6	6	6					
6									9	7	5	8	9	6	4	5	6	9	3	5	4	3	4	3	4	1	5	4	6	4	6					
6										2		2	4	5	7	1	9	8	5	4	1	7	9	8	5	4	5	4	9	9	9					
6													2	6	4	9	3	7	4	9	8	1	5	5				4	9	9	7					
6															9	4	1	8	5	6	9	4	3	7	7	4	3	7	1	8	7					
6																9	3	6	4	5	9	3	6	4	5	9	7	1	4	4	4					
6																	1	8	7	5	9	4	5	9	4	5	3	5	6	9	1					
6																	7	1	8	9	4	5	5	4	5	6	3	9	5	1	5					
6																	5	4	9	6	3	7	4	9	8	1	5	5	4	9	9					
6																	4	9	5	3	6	9	4	3	7	7	4	1	8	4	8					
6																	9	5	4	6	3	2	6	4	9	7	8	4	4	7	8					
6																							2	6	4	9	7	8	4	3	4					
6																								8	1	4	4	4	3	4	4	3				
6																								7	9	9	9	3	4	4	4	3				
6																									1	5	3	7	4	4	4	4	3			
6																									4	7	5	5	6	9	9	9	9			
6																									5	8	9	8	5	6	6	6	6			
6																									9	4	6	1	9	5	9	5	9			
6																										4	1	5	9	9	9	9	9	9		
6																											2	8	7	3	5	5	5	5	5	
6																												9	5	5	5	5	5	5	5	5

$$C 5; \frac{1}{2}^a = \tag{19}$$



$$C 5; \frac{1}{2}^b = \tag{20}$$



Finally,

$$C_{5; \frac{3}{2}} = \quad (21)$$

2	2	2	2	2	3	3	3	2	3	3	3	3	3	2	2	1	1	1	1	2	1	1	1	2	2	2	2	2	4	3			
	3	2	3	2	2	2	2	3	1	3	2	1	3	1	3	3	1	1	2	1	2	3	2	2	2	2	1	4	1	2			
		3	2	2	2	1	3	2	2	3	3	1	3	1	1	3	2	1	1	3	2	2	2	2	2	1	2	1	4	2	7		
			3	1	3	3	1	2	2	1	2	2	3	1	2	2	3	3	1	2	1	3	2	2	3	4	1	2	1	2	7		
			3	1	3	3	1	2	2	1	2	2	3	1	2	2	3	2	1	3	2	2	3	2	3	4	1	1	3	2	7		
				3	1	2	2	1	2	1	2	1	3	1	2	3	2	3	2	2	3	2	1	4	1	3	2	2	2	1	7		
					3	2	1	2	1	3	1	2	2	2	3	2	3	1	1	4	2	2	3	2	3	4	1	2	3	1	7		
						3	1	1	2	2	2	2	2	2	2	3	3	4	1	1	2	2	3	3	1	1	2	3	1	1	7		
							3	1	2	1	2	2	2	2	3	1	3	1	2	4	3	2	2	4	3	2	2	1	3	2	1	7	
								2	1	2	2	2	3	2	2	3	2	4	2	3	3	1	2	3	2	3	1	2	3	1	1	7	
									2	1	2	2	3	2	2	3	2	4	3	1	3	3	2	3	2	3	2	2	2	1	1	7	
										3	1	3	4	1	3	2	2	3	2	2	3	2	2	3	2	2	3	1	3	1	1	7	
											1	1	4	1	4	2	3	2	2	3	3	2	2	3	2	2	1	3	1	1	1	7	
												4	3	1	2	2	2	2	2	3	1	1	4	2	2	2	3	1	1	3	1	2	7
														1	3	2	2	2	2	2	1	3	3	1	1	3	1	1	3	2	:	7	
															2	1	2	1	2	2	1	2	2	1	2	2	1	3	3	2	7		
															2	1	2	2	1	1	2	2	2	3	1	3	2	3	3	2	7		
																1	3	1	1	3	2	1	1	3	3	2	1	3	2	7			
																	2	1	3	2	2	1	1	3	3	2	1	3	2	7			
																		2	2	1	3	2	2	1	3	2	2	1	3	2	7		
																			1	2	2	3	1	2	3	1	2	2	3	2	7		
																				3	3	1	2	2	3	2	3	2	3	2	7		
																					3	2	2	3	2	3	2	3	2	7			
																						3	2	2	3	2	2	5	2	7			
																															2		

A cknow ledgm ents

We are indebted to M .W ierzbowska, G .Santoro, E .Tosatti for useful discussions. This work was supported by the European Union, contract ERBFM - RXCT 970155 (TMR FULPROP), covering in particular the postdoctoral work of M .Luders, and by MURST COFIN 01.

R eferences

- [1] M .Luders, A .Bordon, N .M anini, A .Dal Corso, M .Fabrizio, and E .Tosatti, *Philos.M ag.B* 82, 1611 (2002).
- [2] A .M .Panich, P .K .Umm at, and W .R .Datars, *Solid State Comm un.* 121, 367 (2002).
- [3] A .Ceulemans, and P .W .Fowler, *J.Chem .Phys.* 93, 1221 (1990).
- [4] N .M anini and P .De Los Rios, *Phys.Rev.B* 62, 29 (2000).
- [5] N .M anini and E .Tosatti, *Phys.Rev.B* 58, 782 (1998).

- [6] N. Manini, A. Dal Corso, M. Fabrizio, and E. Tosatti, *Philos. Mag. B* 81, 793 (2001).
- [7] P. H. Butler, *Point Group Symmetry Applications* (Plenum, New York, 1981).
- [8] E. Tosatti, N. Manini, and O. Gunnarsson, *Phys. Rev. B* 54, 17184 (1996).
- [9] M. Saito, *Phys. Rev. B* 65, 220508 (2002).
- [10] R. Engman, *The Jahn Teller Effect in Molecules and Crystals* (Wiley, London, 1972).
- [11] A. Auerbach, N. Manini, and E. Tosatti, *Phys. Rev. B* 49, 12998 (1994).
- [12] N. Manini and P. De Los Rios, *J. Phys.: Condens. Matter* 10, 8485 (1998).
- [13] V. Brouet, H. Alloul, T. N. Le, S. Garaj, and L. Forro, *Phys. Rev. Lett.* 86, 4680 (2001).
- [14] R. F. Kiehl, T. L. Duty, J. W. Schneider, A. MacFarlane, K. Chow, J. W. Elzey, P. Mendels, G. D. Morris, J. H. Brewer, E. J. Ansaldo, C. Niedermayer, D. R. Noakes, C. E. Stronach, B. Hitti, and J. E. Fischer, *Phys. Rev. Lett.* 69, 2005 (1992).
- [15] G. Zimmer, M. Mehring, C. Goze, and F. Rachdi, in *Physics and Chemistry of Fullerenes and Derivatives*, edited by H. Kuzmany, J. Fink, M. Mehring, and S. Roth (World Scientific, Singapore, 1995), p. 452.
- [16] I. Lukyanchuk, N. Kirova, F. Rachdi, C. Goze, P. Molinie, and M. Mehring, *Phys. Rev. B* 51, 3978 (1995).
- [17] K. Prassides, S. Margadonna, D. Aron, A. Lappas, H. Shimoda, and Y. Iwasa, *J. Am. Chem. Soc.* 121, 11227 (1999).
- [18] A. Schilder, H. Kobs, I. Rystau, W. Schutz, and B. Gotschy *Phys. Rev. Lett.* 73, 1299 (1994).
- [19] D. P. Arovas and A. Auerbach, *Phys. Rev. B* 52, 10114 (1995).
- [20] M. Capone, M. Fabrizio, and E. Tosatti, *Phys. Rev. Lett.* 86, 5361 (2001).
- [21] M. Capone, M. Fabrizio, C. Castellani, and E. Tosatti, *Science* 296, 2364 (2002).
- [22] J. H. Schon, Ch. Kloc, R. C. Haddon, and B. Batlogg, *Science* 288, 656 (2000).